Journal of Biomolecular NMR, 2 (1992) 103–108
ESCOM

J-Bio NMR 051

Improved resolution in three-dimensional constant-time triple resonance NMR spectroscopy of proteins

Arthur G. Palmer III, Wayne J. Fairbrother, John Cavanagh, Peter E. Wright and Mark Rance

Department of Molecular Biology MB-2, The Scripps Research Institute, 10666 North Torrey Pines Road, La Jolla, CA 92037, U.S.A.

Received 24 September 1991
Accepted 21 October 1991

Keywords: 3D NMR; Triple resonance; Proteins; Constant-time; Isotopic labelling; Glucose permease

SUMMARY

Two new protocols for the three-dimensional, triple resonance, constant-time HCA(CO)N NMR experiment are presented that significantly increase the experimental resolution attainable in the C^{α} frequency dimension. Experimental verification of the new experiments is provided by spectra of the IIA domain of glucose permease from *Bacillus subtilis*.

The three-dimensional triple resonance HCA(CO)N NMR experiment establishes backbone sequential connectivities in uniformly ^{13}C and ^{15}N enriched proteins by correlating the H^{α} and C^{α} chemical shifts of one residue with the amide ^{15}N chemical shift of the next residue in the protein sequence (Ikura et al., 1990; Kay et al., 1990). Recently, Powers et al. (1991) introduced a constant-time (Bax and Freeman, 1981; Rance et al., 1984) version of the HCA(CO)N experiment. In this Communication, two modified schemes for the constant-time experiment are described that achieve significant improvement in the spectral resolution in the C^{α} frequency dimension.

Pulse sequences for the new constant-time HCA(CO)N experiments are presented in Fig. 1; relevant phase cycling and experimental parameters are given in the figure legend. The constant-time HCA(CO)N pulse sequence of Powers et al. (1991) is similar to the sequence of Fig. 1a, except that the three 180° pulses during T are applied simultaneously at $(T-t_1)/2$. Following an initial INEPT (Morris and Freeman, 1979) polarization transfer from the H^{α} spin to the C^{α} spin, the product operator (Sørensen et al., 1983; Packer and Wright, 1983; van de Ven and Hilbers, 1983) of interest at the beginning of T is $C^{\alpha}_{y}H^{\alpha}_{z}$ for the original and the new constant-time sequences.

0925-2738/$ 5.00

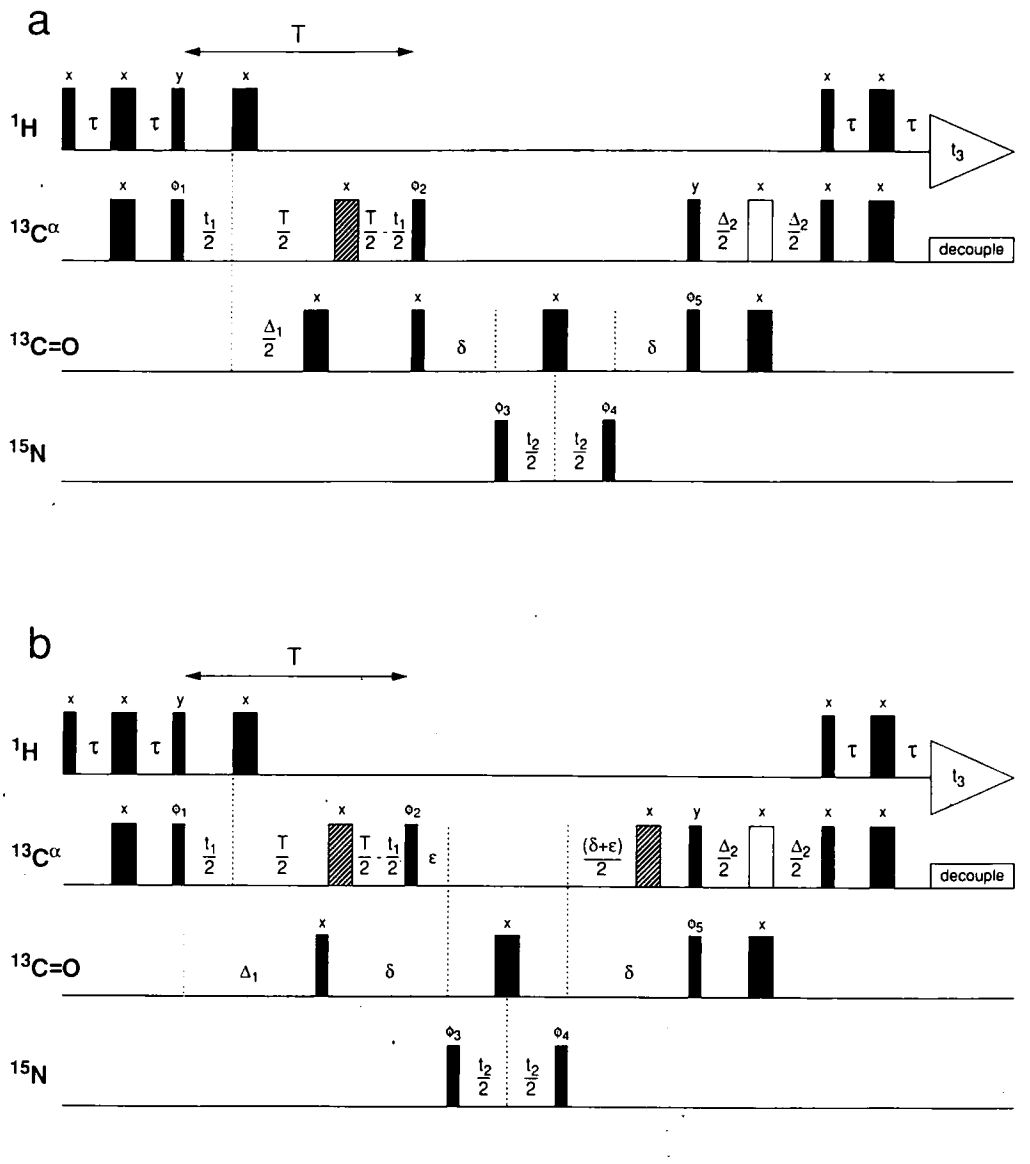

Fig. 1. Pulse schemes for constant-time HCA(CO)N experiments using (a) scheme I and (b) scheme II. Thin and thick bars represent 90° and 180° pulses, respectively. The phase cycling used was $\varphi_1 = x$; $\varphi_2 = 4(y), 4(-y)$; $\varphi_3 = x, -x$; $\varphi_4 = 8(x), 8(-x)$; $\varphi_5 = 2(x), 2(-x)$; receiver = $x, 2(-x), x, -x, 2(x), 2(-x), 2(x), -x, x, 2(-x), x$. Quadrature detection in ω_1 and ω_2 was achieved by cycling the phases of φ_1, φ_3, and the receiver in the States-TPPI manner (Marion et al., 1989). The field strength (specified as the inverse of the 360° pulse length) of the C^{α} and C′ pulses shown as dark bars was adjusted to $\Omega/\sqrt{15}$, in which Ω is the difference between the C^{α} and C′ carrier frequencies; consequently, the C′ spins are minimally excited by pulses applied to the C^{α} spins, and vice versa (Ernst et al., 1987). The field strengths of the C^{α} 180° pulses shown as hatched bars were adjusted to $\Omega/\sqrt{3}$, which ensures inversion of C^{β} spins while minimizing excitation of C′ spins (Ernst et al., 1987). The field strengths of the C^{α} 180° pulses shown as open bars were adjusted to approximately 2 kHz to minimize the effects of the passive $C^{\alpha} - C^{\beta}$ couplings during the interval Δ_2 (Kay et al., 1990). Decoupling of C^{α} spins during acquisition was performed using GARP-1 phase modulation (Shaka et al., 1985). The fixed delays are $\tau = 1/(4J_{H\alpha C\alpha})$, $\Delta_2 = 1/(3J_{C\alpha C'})$ to $1/(2J_{C\alpha C'})$ and $\delta = 1/(3J_{NC'})$ to $1/(2J_{NC'})$.

The evolution of coherence through the constant-time period, T, for the experiment of Powers et al. (1991) is given by

$$C^{\alpha}_{y}H^{\alpha}_{z} \xrightarrow{T} C^{\alpha}_{x}H^{\alpha}_{z}C'_{z}\cos\Omega_{C^{\alpha}}t_1\Gamma(T) \tag{1}$$

in which the coherence transfer function, $\Gamma(T)$, is

$$\Gamma(T) = \sin(\pi J_{C^{\alpha}C'}T)\cos(\pi J_{C^{\alpha}C^{\beta}}T)\cos(\pi J_{H^{\alpha}C^{\alpha}}T) \tag{2}$$

C′ represents the carbonyl carbon spin, $\Omega_{C\alpha}$ is the resonance frequency offset of the C^{α} spin, $J_{C\alpha C'}$ is the scalar coupling constant between the C^{α} and C′ carbon spins, $J_{C\alpha C\beta}$ is the scalar coupling constant between the C^{α} and C^{β} spins, and $J_{H\alpha C\alpha}$ is the scalar coupling constant between the H^{α} and C^{α} spins. As shown by Eq. (2), the H^{α} and C′ spins are coupled to the C^{α} spin for the entirety of T because 180° pulses are applied simultaneously to all three nuclei at $(T-t_1)/2$. The resonance line shape in the ω_1 dimension following Fourier transformation is a singlet centered at the frequency $\Omega_{C\alpha}$; in the original version of the HCA(CO)N experiment the line shape was a multiplet with in-phase and anti-phase contributions from the $C^{\alpha}-C^{\beta}$ and $C^{\alpha}-C'$ scalar couplings (Ikura et al., 1990; Kay et al., 1990).

The value of T critically affects the constant-time HCA(CO)N experiment in three ways: (i) T indirectly determines the resolution obtainable in the ω_1 dimension because the maximum value of t_1 cannot exceed T; (ii) coherence transfer is optimized by selecting T to maximize $\Gamma(T)$; and (iii) the amplitude of the signal is reduced by a factor of $\exp(-RT)$ for all values of t_1, in which R is the average relaxation rate constant for the $C^{\alpha}_{x}H^{\alpha}_{z}C'_{z}$ operator. In the original application of this experiment, a short value of T = 7 ms was employed and the resolution in the final spectrum was enhanced by linear prediction (Powers et al., 1991). In Eq. (2), $\Gamma(T)$ depends on three independent coupling constants but only one time period, T; consequently, extending T to increase the *experimental* resolution in the ω_1 dimension generally is not practical.

In the new schemes for recording constant-time HCA(CO)N experiments (Fig. 1), pulses are applied to the H^{α}, C^{α} and C′ nuclei at different points during T such that the evolution of each scalar coupling to the C^{α} spin depends upon a unique time period. Consequently, the coherence transfer functions for the new sequences can be optimized independently with respect to each scalar coupling constant. As a result, T can be extended to achieve higher resolution in the ω_1 dimension.

For the pulse sequence of Fig. 1a (scheme I), the evolution of coherence during T is given by

$$C^{\alpha}_{y}H^{\alpha}_{z} \xrightarrow{T} C^{\alpha}_{x}H^{\alpha}_{z}C'_{z}\cos\Omega_{C^{\alpha}}t_1\,\Gamma_I(\Delta_1,T) \tag{3}$$

in which $\Gamma_I(\Delta_1,T)$ is the coherence transfer function:

$$\Gamma_I(\Delta_1,T) = \sin(\pi J_{C^{\alpha}C'}\Delta_1)\cos(\pi J_{C^{\alpha}C^{\beta}}T) \tag{4}$$

Although not included in Eq. (3), unresolved scalar couplings between the C^{α} spin and ^{15}N amide

spins in the same and succeeding residues slightly broaden the resonance signal; decoupling during t_1 can be achieved if desired by application of a 180° pulse to the ^{15}N spins at the same time as the 180° pulse is applied to the proton spins during T.

In the experiment of Powers et al. (1991) and in scheme I, a delay, δ, immediately follows T during which the C′ coherence of one residue becomes anti-phase with respect to the amide ^{15}N spin of the next residue in the sequence as a result of the scalar coupling between the two spins. To shorten the overall duration of the constant-time HCA(CO)N experiment and reduce signal loss due to relaxation, the pulse sequence, scheme II, of Fig. 1b was developed that overlaps the delay, δ, and the constant-time period, T. The value of ε can be positive or negative, which allows $\Delta_1 + \delta$ to be greater or less than T. For $\varepsilon \geqslant 0$, the evolution during $T + \varepsilon$ is:

$$C^{\alpha}_{y}H^{\alpha}_{z} \xrightarrow{T} C^{\alpha}_{x}H^{\alpha}_{z}C'_{x}N_{z}\cos \Omega_{C'}t_1 \; \Gamma_{II}(\Delta_1,\delta,T) \tag{5}$$

in which the coherence transfer function $\Gamma_{II}(\Delta_1,\delta,T)$ is

$$\Gamma_{II}(\Delta_1,\delta,T) = \sin(\pi J_{C^{\alpha}C'}\Delta_1)\cos(\pi J_{C^{\alpha}C^{\beta}}T)\sin(\pi J_{NC'}\delta) \tag{6}$$

N represents the amide ^{15}N spin and $J_{NC'}$ is the scalar coupling constant for the N and C′ spins. Following the 90° pulse on the C′ spin, the spin system is in multiple-quantum coherence with respect to the C^{α} and C′ spins for the duration of T; chemical-shift evolution of the C'_x operator during δ is refocused by the 180° pulse in the middle of the t_2 period and has not been included in Eq. (6). Unlike scheme I and the experiment of Powers et al. (1991), ^{15}N decoupling cannot be obtained during t_1. Similar results are obtained for $\varepsilon < 0$, except that evolution of the transverse ^{15}N operator must be considered.

In contrast to Eq. (2), the right-hand sides of Eqs. (4) and (6) do not depend upon $J_{H\alpha C\alpha}$, and the trigonometric functions of coupling constants $J_{C\alpha C'}$, $J_{C\alpha C\beta}$ and $J_{NC'}$ depend upon the independent time periods Δ_1, T and δ respectively. The time periods Δ_1 and δ can be set to optimize the appropriate trigonometric factors in Eqs. (4) and (6) separately; therefore, the coherence transfer functions depend primarily on $\cos(\pi J_{C\alpha C\beta}T)$, and subject to relaxation losses, T can be extended to increase the experimental resolution in the ω_1 dimension. Additionally, the magnitudes of the coherence transfer for schemes I and II are equal to or greater than the transfer function for the experiment of Powers et al. (1991) for all values of T. If T is chosen such that $\cos(\pi J_{C\alpha C\beta}T) < 0$, the resonances arising from glycine residues, which lack a C^{β} coupling partner, will be inverted relative to the other resonances. If $T = \Delta_1 = 7$ ms and $\varepsilon = \delta$, schemes I and II are essentially equivalent to the constant-time experiment of Powers et al. (1991).

To compare the different constant-time HCA(CO)N experiments, three spectra of the uniformly $^{13}C/^{15}N$ labelled IIA domain of the glucose permease from *Bacillus subtilis* (IIA^{glc}, 162 residues, 17.4 kDa) (Fairbrother et al., 1991) were recorded using the pulse sequences of Fig. 1. The protein sample was 2 mM in D_2O at pH 6.6 and experiments were performed at 308 K. The first spectrum was recorded by using the pulse sequence of scheme I with T = 7 ms. The second and third spectra were obtained by using the pulse sequences of schemes I and II, respectively, with T = 27 ms.

Spectra were recorded using a Bruker AMX-500 NMR spectrometer equipped with a three-channel interface. The radiofrequency (RF) pulses for the ^1H, aliphatic ^{13}C, and ^{15}N frequencies

were generated using the proton, X-nucleus, and Y-nucleus channels of the spectrometer. Pulses for the carbonyl ^{13}C frequency range were generated by using a frequency synthesizer (PTS300, Programmed Test Sources) and a pulse amplifier (M3205, American Microwave Technology, Inc.). A digital word generator (RS670, Interface Technology) was used to control the RF phase of the synthesizer and a home-built switch was used to gate the output of the synthesizer. Data processing in the ω_1 and ω_3 dimensions was performed using FTNMR (Hare Research, Inc.); a separate FORTRAN routine was used for processing in the ω_2 dimension.

Figure 2 shows sections of two-dimensional (ω_1,ω_3) slices from the three HCA(CO)N spectra. The slices are taken at a ^{15}N chemical shift of 121.2 ppm; the ω_1 and ω_3 dimensions display the C^α and H^α shifts, respectively. The increase in resolution in the ω_1 dimension is clearly evident for the spectra recorded with T = 27 ms (Figs. 2b,c) compared to the spectrum recorded with T = 7 ms (Fig. 2a): three of the cross peaks in Fig. 2a are resolved into two peaks each in Figs. 2b and 2c. The signal-to-noise ratios of the three spectra are illustrated in Fig. 3, which shows cross sections taken parallel to the ω_3 dimension through the resonances for valine 52 (Fig. 3a), serine 101 (Fig. 3b) and threonine 141 (Fig. 3c). As a consequence of the reduced line widths in the ω_1 dimension and the somewhat longer acquisition times, the spectrum acquired with scheme II and T = 27 ms (upper traces) has a signal-to-noise ratio similar to that of the spectrum acquired with T = 7 ms (lower traces), despite additional relaxation losses during the longer constant-time period. Depending on the particular cross peak, the sensitivity of scheme II, which overlaps T and δ (upper traces), is as much as 40% greater than scheme I (middle traces).

To summarize, two new constant-time HCA(CO)N experiments have been introduced which allow spectra to be recorded with improved resolution in the ω_1 dimension by lengthening the

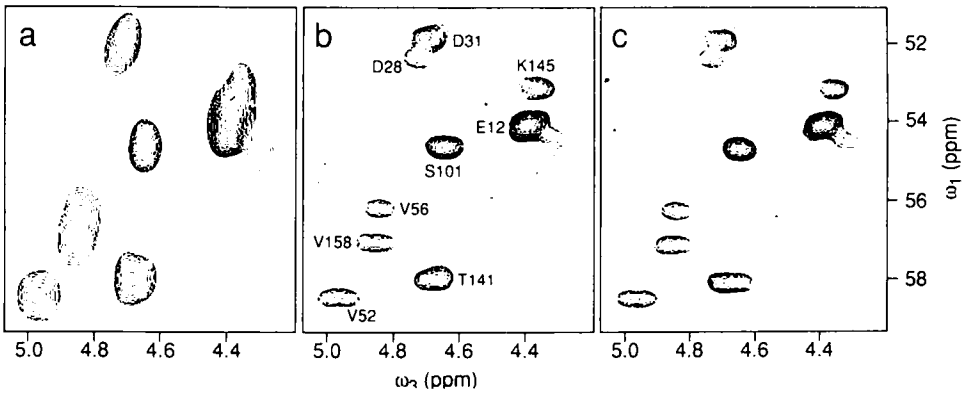

Fig. 2. Sections of (ω_1,ω_3) slices of the HCA(CO)N spectra of IIA^{glc} acquired using (a) scheme I with $T = \Delta_1 = 7$ ms, (b) scheme I with T = 27 ms and $\Delta_1 = 9$ ms, and (c) scheme II with T = 27 ms, $\Delta_1 = 9$ ms and $\varepsilon = 0$. The other delays were $\tau = 1.75$ ms, $\Delta_2 = 6$ ms and $\delta = 18$ ms. The spectral widths were 3.33, 1.75 and 12.5 kHz in ω_1, ω_2 and ω_3, respectively. The proton, aliphatic carbon, carbonyl and nitrogen carrier frequencies were set to 4.7 ppm, 52.5 ppm, 177 ppm and 116 ppm, respectively. The nominal values of the scalar coupling constants were assumed to be: $J_{C^\alpha C'} = 55$ Hz, $J_{C^\alpha C^\beta} = 37$ Hz, $J_{H^\alpha C^\alpha} = 140$ Hz and $J_{NC'} = 15$ Hz. Spectrum (a) was acquired as 22 complex $t_1 \times 32$ complex $t_2 \times 512$ complex t_3 data points. Thirty two scans were acquired per free induction decay. The spectrum was acquired in 28 h. Spectra (b) and (c) were acquired as 58 complex $t_1 \times 32$ complex $t_2 \times 512$ complex t_3 data points. Sixteen scans were acquired per free induction decay. Each spectrum was recorded in 40 h. The peak labels correspond to the amino acid residues whose H^α and C^α resonances show sequential connectivities to the amide ^{15}N of the following residues with a resonance frequency of approximately 121.9 ppm (allowing for the deuterium isotope shift).

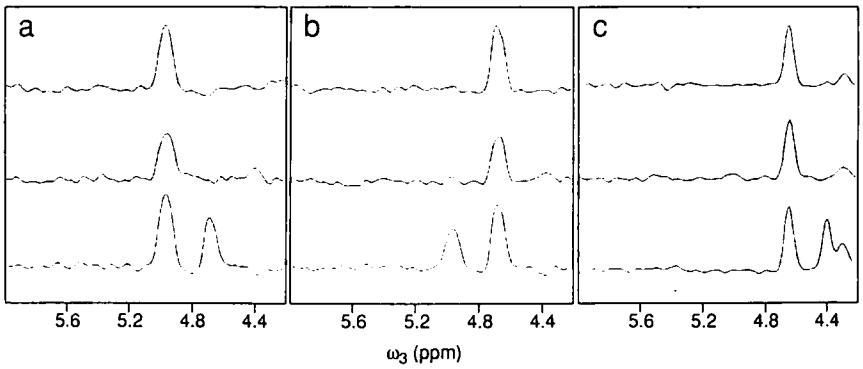

Fig. 3. Cross sections through the cross peaks of (a) valine 52, (b) serine 101 and (c) threonine 141 for the spectra of Fig. 2. The lower, middle and upper cross sections in each part of the figure correspond to the spectra shown in Figs. 2a, 2b and 2c, respectively. The cross sections shown for the spectrum of Fig. 2a (pulse scheme I, T = 7 ms) have been multiplied by a factor of 3.88 to equalize the noise level in all three spectra.

constant-time period. Increased resolution is accompanied inevitably by decreased sensitivity due to relaxation losses; however, as shown experimentally, spectra with satisfactory signal-to-noise ratios can be acquired feasibly with either of the new experiments. The second pulse sequence is more sensitive than the first sequence and is usually the method of choice, unless ^{15}N decoupling during the t_1 period is desired. The constant-time period used in the first scheme also can be used to obtain improved resolution in the constant-time HCACO experiment (Powers et al., 1991).

ACKNOWLEDGEMENTS

This work was supported in part by grants from the National Science Foundation (DMB 8903777) and the National Institutes of Health (GM-36643). W.J.F. was supported by a Damon Runyon-Walter Winchell Cancer Research Fund Postdoctoral Fellowship (DRG-1059). The IIA^{glc} sample was kindly provided by Drs. J. Reizer and M.H. Saier Jr. (University of California at San Diego).

REFERENCES

Bax, A. and Freeman, R. (1981) *J. Magn. Reson.*, **44**, 542–561.
Ernst, R.R., Bodenhausen, G. and Wokaun, A. (1987) *Principles of Nuclear Magnetic Resonance in One and Two Dimensions*, Clarendon Press, Oxford, pp. 119–124.
Fairbrother, W.J., Cavanagh, J., Dyson, H.J., Palmer, A.G., Sutrina, S.L., Reizer, J., Saier, M.H. and Wright, P.E. (1991) *Biochemistry*, **30**, 6896–6907.
Ikura, M., Kay, L.E. and Bax, A. (1990) *Biochemistry*, **29**, 4659–4667.
Kay, L.E., Ikura, M., Tschudin, R. and Bax, A. (1990) *J. Magn. Reson.*, **89**, 496–514.
Marion, D., Ikura, M., Tschudin, R. and Bax, A. (1989) *J. Magn. Reson.*, **85**, 393–399.
Morris, G.A. and Freeman, R. (1979) *J. Am. Chem. Soc.*, **101**, 760–762.
Packer, K.J. and Wright, K.M. (1983) *Mol. Phys.*, **50**, 797–813.
Powers, R., Gronenborn, A.M., Clore, G.M. and Bax, A. (1991) *J. Magn. Reson.*, **94**, 209–213.
Rance, M., Wagner, G., Sørensen, O.W., Wüthrich, K. and Ernst, R.R. (1984) *J. Magn. Reson.*, **59**, 250–261.
Shaka, A.J., Barker, P.B. and Freeman, R. (1985) *J. Magn. Reson.*, **64**, 547–552.
Sørensen, O.W., Eich, G., Levitt, M.H., Bodenhausen, G. and Ernst, R.R. (1983) *Prog. NMR Spectrosc.*, **16**, 163–192.
van de Ven, F.J.M. and Hilbers, C.W. (1983) *J. Magn. Reson.*, **54**, 512–520.